NACA

RESEARCH MEMORANDUM

EFFECTS OF SOME AIRFOIL-SECTION VARIATIONS ON WING-AILERON ROLLING EFFECTIVENESS AND DRAG AS DETERMINED IN FREE FLIGHT AT TRANSONIC AND SUPERSONIC SPEEDS

By

Carl A. Sandahl, William M. Bland, Jr., and H. Kurt Strass

Langley Aeronautical Laboratory
Langley Air Force Base, Va.

NATIONAL ADVISORY COMMITTEE FOR AERONAUTICS

WASHINGTON
July 22, 1949

Classification cancelled (or changed to) Unclassified

By Authority of NASA Tech Pub Announcement #79

(OFFICER AUTHORIZED TO CHANGE)

13 Apr 66

By

(GRADE OF OFFICER MAKING CHANGE)

6 Apr 66

DATE

NATIONAL ADVISORY COMMITTEE FOR AERONAUTICS

RESEARCH MEMORANDUM

EFFECTS OF SOME AIRFOIL-SECTION VARIATIONS ON WING-AILERON ROLLING EFFECTIVENESS AND DRAG AS DETERMINED IN FREE FLIGHT AT TRANSONIC AND SUPERSONIC SPEEDS

By Carl A. Sandahl, William M. Bland, Jr., and H. Kurt Strass

SUMMARY

An experimental investigation has been made in free flight of the rolling effectiveness of plain ailerons in conjunction with wings having 0° and 45° sweepback employing several airfoil sections. The total drag of the test vehicles was also obtained. Positive control effectiveness over the Mach number range investigated was obtained for the configurations which employed airfoil sections with trailing-edge angles of the order of 10°. Reversal of effectiveness was encountered for configurations with trailing-edge angles of the order of 20°. The aileron effectiveness was not appreciably affected by changes in the shape of the forward part of the airfoil section. For the rectangular wings near Mach numbers of unity, the blunt-nose sections had slightly lower drag than did the sharp-nose sections. At higher supersonic Mach numbers the drag of the rectangular wings having sharp-nose sections approached that of the sweptback wings. For the sweptback wings, variations of airfoil section produced no measurable differences in drag for the Mach number range investigated.

INTRODUCTION

At the present time the Pilotless Aircraft Research Division of the Langley Laboratory is engaged in an investigation of wing-aileron rolling-effectiveness characteristics at transonic and supersonic speeds utilizing rocket-propelled test vehicles in free flight. A considerable amount of systematic experimental information relating to plain ailerons on wings of various plan forms having NACA 65009 airfoil sections has been obtained by the techniques described in references 1 and 2. The results obtained have been summarized in reference 3.

In order to evaluate the effects of some major variations in airfoil section on the rolling effectiveness of plain ailerons, tests were made of configurations having NACA 65A009, NACA 16-009, symmetrical double-wedge and circular-arc airfoil sections of 9-percent thickness ratio. These four sections were tested with wings of aspect ratio 3.71,

taper ratio 1.0 having 0° and 45° sweepback. The purpose of this paper is to present these additional results.

The tests were made by means of the technique described in reference 1 which permits the evaluation of the wing-aileron rolling effectiveness continuously over the Mach number range from about 0.6 to 1.9 at relatively large scale. The variation of total drag coefficient with Mach number was also obtained.

SYMBOLS

$\frac{pb}{2V}$	wing-tip helix angle, radians
p	rolling velocity, radians per second
b	diameter of circle swept by wing tips, feet
V	flight-path velocity, feet per second
C_D	total drag coefficient based on exposed wing area (1.563 sq ft)
M	Mach number
R	Reynolds number based on wing chord (0.59 ft)
A	aspect ratio $\left(\frac{b}{c}\right)$
c	chord of wing parallel to model center line, feet
δ_a	deflection of each aileron measured in plane normal to chord plane and parallel to fuselage center line, degrees (see fig. 1(b))
i_w	wing incidence measured in plane of δ_a, degrees (see fig. 1(b))

TEST VEHICLES AND TESTS

The general arrangement of the test vehicles is shown in figures 1 and 2. Additional pertinent information is contained in tables I and II.

The test vehicles, which were relatively simple, inexpensive, and expendable, consisted of a pointed cylindrical wooden body to which the particular wing-aileron configuration under investigation was attached in a three-panel arrangement. Unpublished tests of three- and four-panel arrangements indicate that, with regard to the rolling-effectiveness

characteristics, the interference effects between the wings were negligible. Several test vehicles, differing nominally only in the aileron deflection, of each configuration were tested. The models were finished with clear lacquer and were smooth and fair.

The wings were constructed of laminated wood and were stiffened by means of steel plates cycle-welded into the upper and lower wing surfaces as shown in figure 1. The outer surfaces of the steel plates were covered with a wood veneer to facilitate construction. In order to establish that this construction possessed sufficient stiffness to minimize the effects of wing twisting, several test vehicles of configurations 50 ($\Lambda = 0^\circ$) and 53 ($\Lambda = 45^\circ$) (see table II) having reduced wing stiffness were constructed. The reduction in wing stiffness was obtained by reducing the thickness of the steel stiffening plates and by using plates of duralumin of reduced thickness. In this way, the wing stiffness was progressively reduced to about one-third of that of the wings employed in the present tests. The results of the flight tests showed no measurable variation of rolling effectiveness with wing stiffness for the range of stiffness values investigated indicating that the effects of wing twisting on the present experimental results are negligible.

The wings were constructed with the aft 20 percent of the airfoil sections deflected to the desired settings. This method of construction simulated plain, sealed, full-span ailerons. The measured values of aileron deflection and wing incidence are estimated to be within $\pm 0.1^\circ$ and $\pm 0.05^\circ$, respectively, of the actual values.

The test vehicles were propelled by a two-stage rocket-propulsion system to a Mach number of about 1.9. During coasting flight following burnout of the rocket motor, time histories of the rolling velocity produced by the ailerons (obtained by means of a small radio transmitter designated "spinsonde" contained in the nose of the test vehicles) and the flight-path velocity (obtained by Doppler radar) were recorded. These data, in conjunction with atmospheric data obtained by means of radiosonde, permitted the evaluation of the wing-aileron rolling-effectiveness parameter $\frac{pb}{2V}$ as a function of Mach number. The drag coefficient was also obtained by a process involving a graphical differentiation of the flight-path velocity-time relation. The scale of the tests is indicated by the curves of Reynolds number versus Mach number in figure 3. A more complete description of the technique is given in references 1 and 2.

ACCURACY

The accuracy of the test results is estimated to be within the following limits:

$\frac{pb/2V}{\delta_a}$	(reproducibility of results from supposedly identical models)	±0.001
$\frac{pb/2V}{\delta_a}$	(accuracy of results for any one model owing to limitations on instrumentation)	±0.0001
C_D		±0.002
M		±0.01

Because the measurement of the rolling velocity of the test vehicles is made while the rolling velocity is changing, the measured values of $\frac{pb}{2V}$ differ from steady-roll values. As described in reference 1, the measured values can be corrected to steady-roll values by a relation involving the moment of inertia about the roll axis, the rolling acceleration, and the damping in roll. In figure 4 are shown the measured and corrected variations of $\frac{pb}{2V}$ with Mach number for the configuration from the present tests for which the correction to steady-state conditions was largest. In making the correction an arbitrary value of -0.2 for the damping-in-roll derivative was used over the entire Mach number range. The value of -0.2 is very approximate and is probably conservative; it was chosen simply to illustrate that the magnitude of the correction is negligible for any reasonable value of the damping-in-roll derivative. Consequently, the data presented herein have not been corrected to steady-roll conditions.

RESULTS AND DISCUSSION

The experimental results of the present investigation are given in figures 5 and 6 as curves of the wing-tip helix angle $\frac{pb}{2V}$ and total drag coefficient C_D against Mach number. The wing-aileron rolling-effectiveness characteristics of the configurations tested are summarized in figure 7 as curves of $\frac{pb}{2V}/\delta_a$ versus Mach number. The results in figure 7 have been corrected to zero wing incidence by means of an empirical relation between wing incidence and wing-tip helix angle. This relation was obtained by flight testing several configurations similar to those of the present tests except that the wings were set at 4° incidence and the ailerons were undeflected. These flight tests indicated that the increment in $\frac{pb}{2V}$ due to wing incidence was equal to 1.5 times the angle of incidence in radians for the Mach number range of the present tests.

Rolling characteristics of the rectangular-wing configurations.- The wing-aileron rolling-effectiveness characteristics for the rectangular-wing configurations summarized in figure 7(a) show that, at the lowest Mach numbers investigated and at any Mach number in excess of about 1.2, the rolling effectiveness is of the same order for all configurations tested. However, in the Mach number range from 0.88 to 0.93, reversal of effectiveness for the deflections tested is shown for the configurations having the airfoil sections with the larger trailing-edge angles, that is, the NACA 16-009 and the 9-percent-thick circular arc. In the corresponding Mach number range, reversal is not shown for the configurations having the NACA 65A009 and the 9-percent-thick double-wedge airfoil sections both of which have smaller trailing-edge angles. Comparison of the results for the NACA 65A009 section with those for the double-wedge airfoil section indicates that the variation of effectiveness with Mach number is primarily related to the trailing-edge angle and not to the shape of the forward part of the airfoil section. Comparison of the results for the NACA 16-009 and the circular-arc airfoil sections indicates the same relation.

Rolling characteristics of the sweptback-wing configurations.- The results in figure 7(b) for the swept-wing configuration show that the configurations having the smaller trailing-edge angles exhibit a gradual variation of effectiveness over the Mach number range investigated. For the models employing the NACA 65A009 and the double-wedge airfoil sections the values of $\frac{pb}{2V}/\delta_a$, which are presented for several aileron deflections, agree randomly within the limits of reproducibility of the test results indicating a reasonably linear variation of rolling effectiveness with aileron deflection over the range of deflections tested. The rolling effectiveness of the configurations employing the NACA 16-009 and circular-arc airfoil sections is nonlinear with deflection and is reversed for the smaller deflections over a relatively large supersonic Mach number range. The Mach number range over which reversal occurs is much larger for the swept wings than for the unswept wings.

Drag measurements.- The variation of total drag coefficient with Mach number for the models tested is summarized in figure 8. The curves in figure 8 were obtained by averaging arithmetically the drag of all the models of each configuration presented in figures 5 and 6. It should be noted that the total drag measurements are influenced by section angle-of-attack distribution due to the rolling velocity, aileron deflection, and by unknown interference effects.

The results for the rectangular wings presented in figure 8(a) show that the sharp-nose sections have markedly less drag than the blunt-nose sections at the higher Mach numbers investigated. At Mach numbers approaching 1.7, the drag of the rectangular wings with the double-wedge section approaches that of the wings having 45° sweepback. For the rectangular wings in the vicinity of Mach number 1, the blunt-nose sections have slightly less drag than do the sharp-nose sections. The

drag rise of the double-wedge sections on the rectangular wings occurs at lower Mach numbers than for the other sections tested. The higher drag of this section at high subsonic Mach numbers is probably due to boundary-layer separation induced by the abrupt change of direction of the upper and lower surfaces at the midchord point.

The results for the sweptback configuration given in figure 8(b) are coincident within the experimental accuracy indicating that, for the Mach number range investigated, the effects of airfoil section on the drag of wings having 45° sweep are small.

CONCLUSIONS

The main conclusions based on the results of the present investigation may be stated as follows:

1. Reversal of rolling effectiveness of plain ailerons on the rectangular wings was obtained for trailing-edge angles of the order of 20° in the Mach number range from about 0.88 to 0.93. Reversal was not obtained for trailing-edge angles of the order of 10°.

2. Reversal of effectiveness of plain ailerons on the swept wings was obtained for trailing-edge angles of the order of 20° over a relatively large Mach number range. Reversal was not obtained for trailing-edge angles of the order of 10°.

3. The aileron effectiveness was not appreciably affected by changes in the shape of the forward part of the airfoil section.

4. For the rectangular wings near Mach numbers of unity, the blunt-nose airfoil sections had slightly lower drag than did the sharp-nose sections. At the higher supersonic Mach numbers investigated, the sharp-nose airfoil sections had considerably less drag than did the blunt-nose sections.

5. At Mach number 1.7, the drag of the unswept wing having the symmetrical double-wedge section was equal to that of the wings having 45° sweepback.

6. For the sweptback wings, the various airfoil sections investigated produced no measurable differences in drag in the Mach number range investigated.

Langley Aeronautical Laboratory
National Advisory Committee for Aeronautics
Langley Air Force Base, Va.

[redacted]

REFERENCES

1. Sandahl, Carl A., and Marino, Alfred A.: Free-Flight Investigation of Control Effectiveness of Full-Span 0.2-Chord Plain Ailerons at High Subsonic, Transonic, and Supersonic Speeds to Determine Some Effects of Section Thickness and Wing Sweepback. NACA RM No. L7D02, 1947.

2. Sandahl, Carl A.: Free Flight Investigation of Control Effectiveness of Full-Span, 0.2-Chord Plain Ailerons at High Subsonic, Transonic, and Supersonic Speeds to Determine Some Effects of Wing Sweepback, Taper, Aspect Ratio, and Section Thickness Ratio. NACA RM No. L7F30, 1947.

3. Sandahl, Carl A., and Strass, H. Kurt: Additional Results in a Free-Flight Investigation of Control Effectiveness of Full-Span, 0.2-Chord Plain Ailerons at High Subsonic, Transonic, and Supersonic Speeds to Determine Some Effects of Wing Sweepback, Aspect Ratio, Taper, and Section Thickness Ratio. NACA RM No. L7L01, 1948.

TABLE I

PHYSICAL CHARACTERISTICS OF ALL TEST VEHICLES

Total exposed wing area, sq ft	1.563
Aspect ratio, A	3.71
Taper ratio	1.00
Ratio of aileron span to exposed wing span	1.00
Ratio of aileron span to total wing span	0.81
Ratio of aileron chord to wing chord	0.20
Moment of inertia about center line of test vehicle, slug-ft^2	0.10

TABLE II

PHYSICAL CHARACTERISTICS OF CONFIGURATION TESTED

Configuration	Wing sweepback (deg)	[a]NACA airfoil section	[d]Nominal trailing-edge angle (deg)
50	0	65A009	10.6
115	0	16-009	21.0
119	0	(b)	10.2
117	0	(c)	20.4
53	45	65A009	10.6
116	45	16-009	21.0
120	45	(b)	10.2
118	45	(c)	20.4

[a]In plane parallel to test vehicle center line.

[b]Double-wedge section of 9-percent-thickness ratio symmetrical with respect to chord line and to line normal to chord line at midchord point.

[c]Circular-arc section of 9-percent-thickness ratio symmetrical with respect to chord line and to line normal to chord line at midchord point.

[d]In plane parallel to test vehicle center line. Actual measured values agreed with nominal values within $\pm 0.2^{\circ}$.

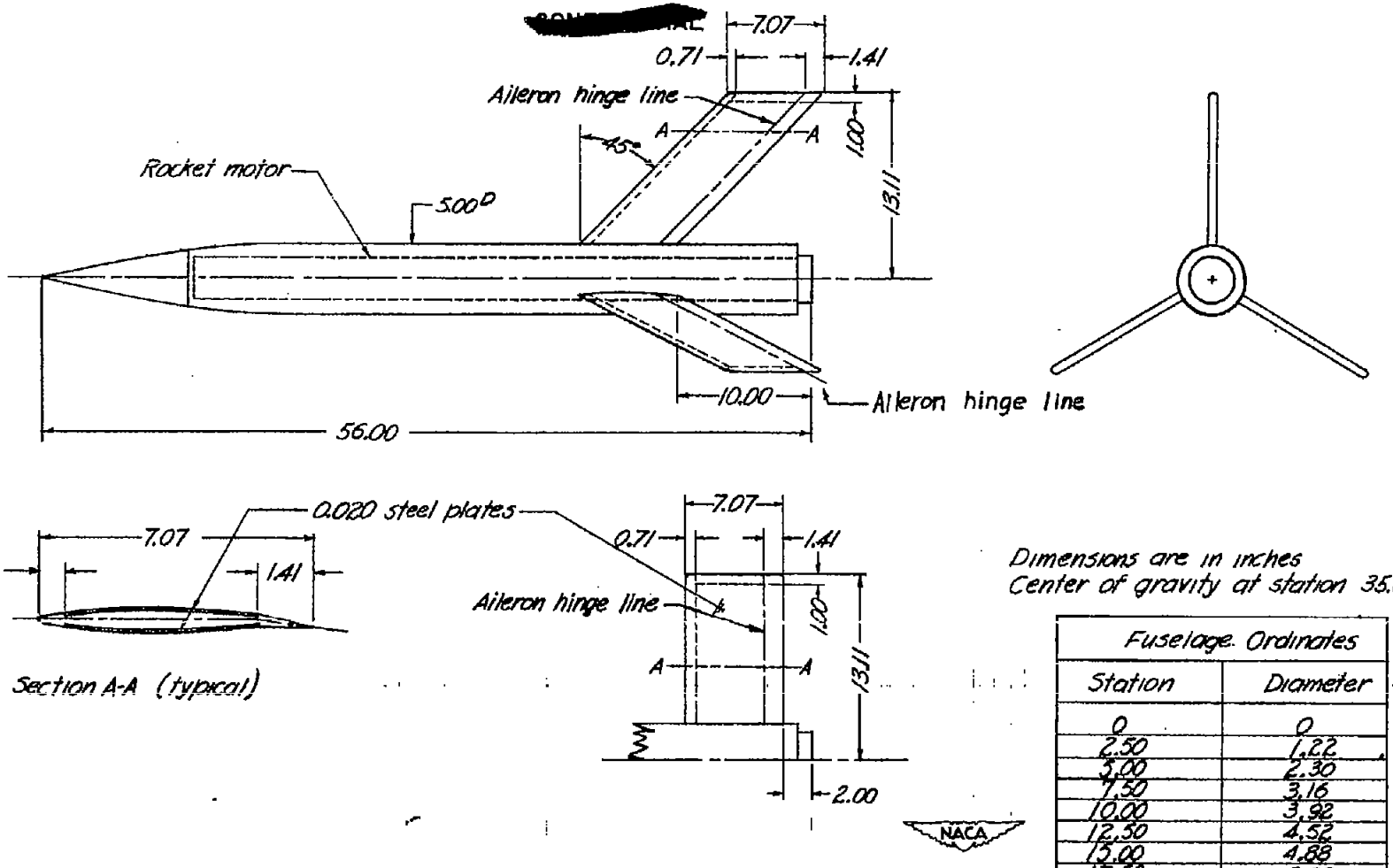

Fuselage. Ordinates	
Station	Diameter
0	0
2.50	1.22
5.00	2.30
7.50	3.16
10.00	3.92
12.50	4.52
15.00	4.88
17.50	5.00

(a) Geometric details.

Figure 1.— General arrangement of test vehicles.

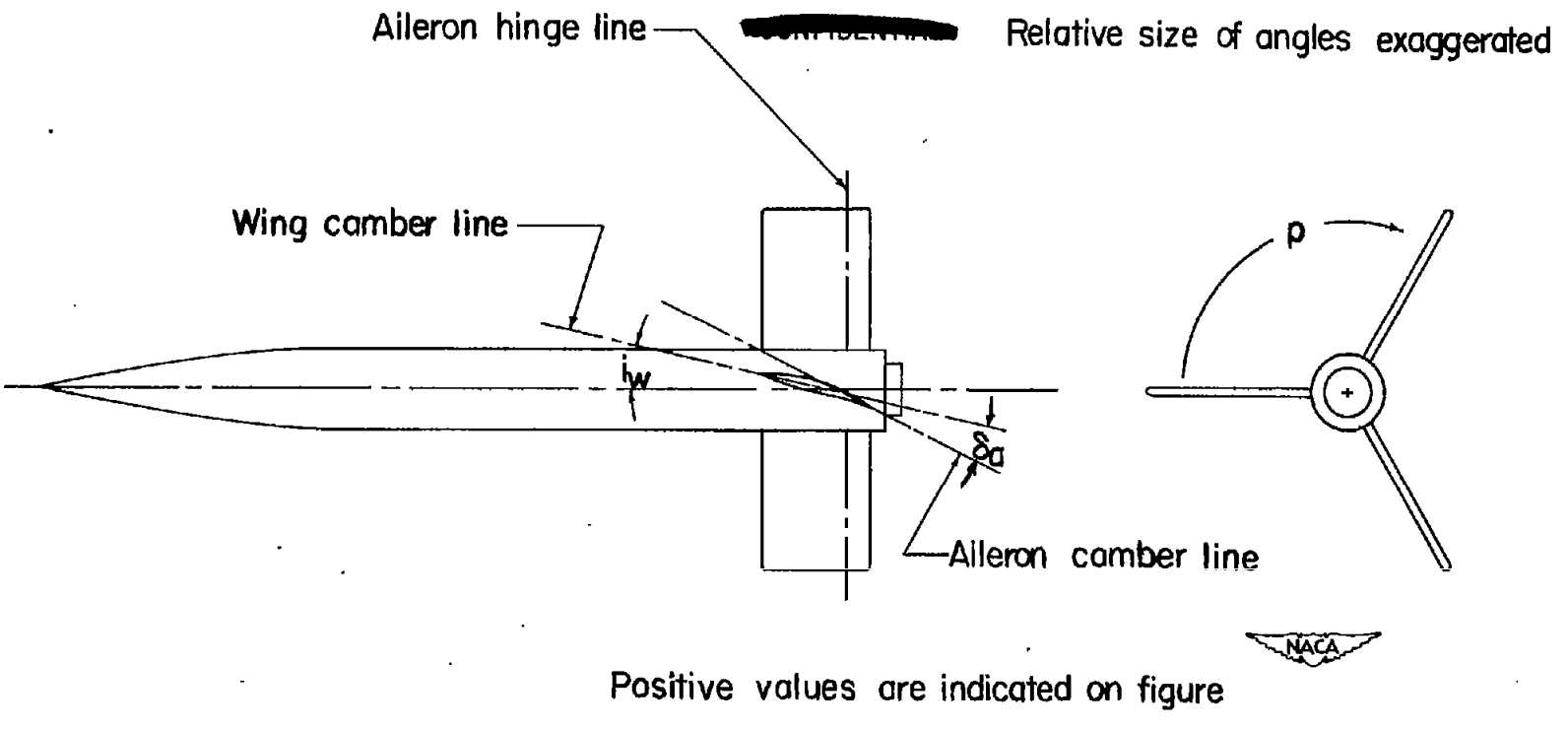

(b) Sign conventions.

Figure 1.– Concluded.

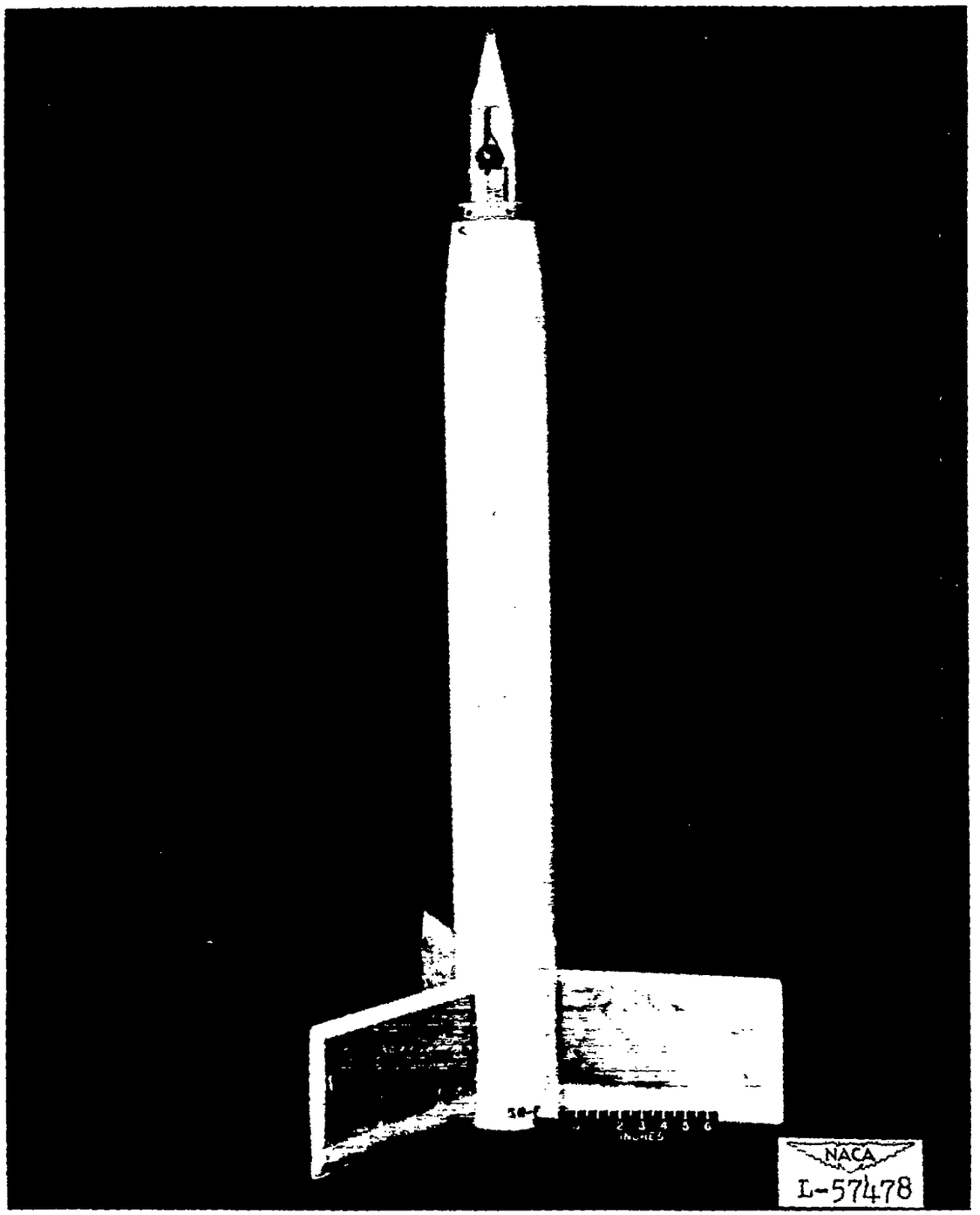

(a) $\Lambda = 0^{\circ}$.

Figure 2.- Photographs of typical test vehicles.

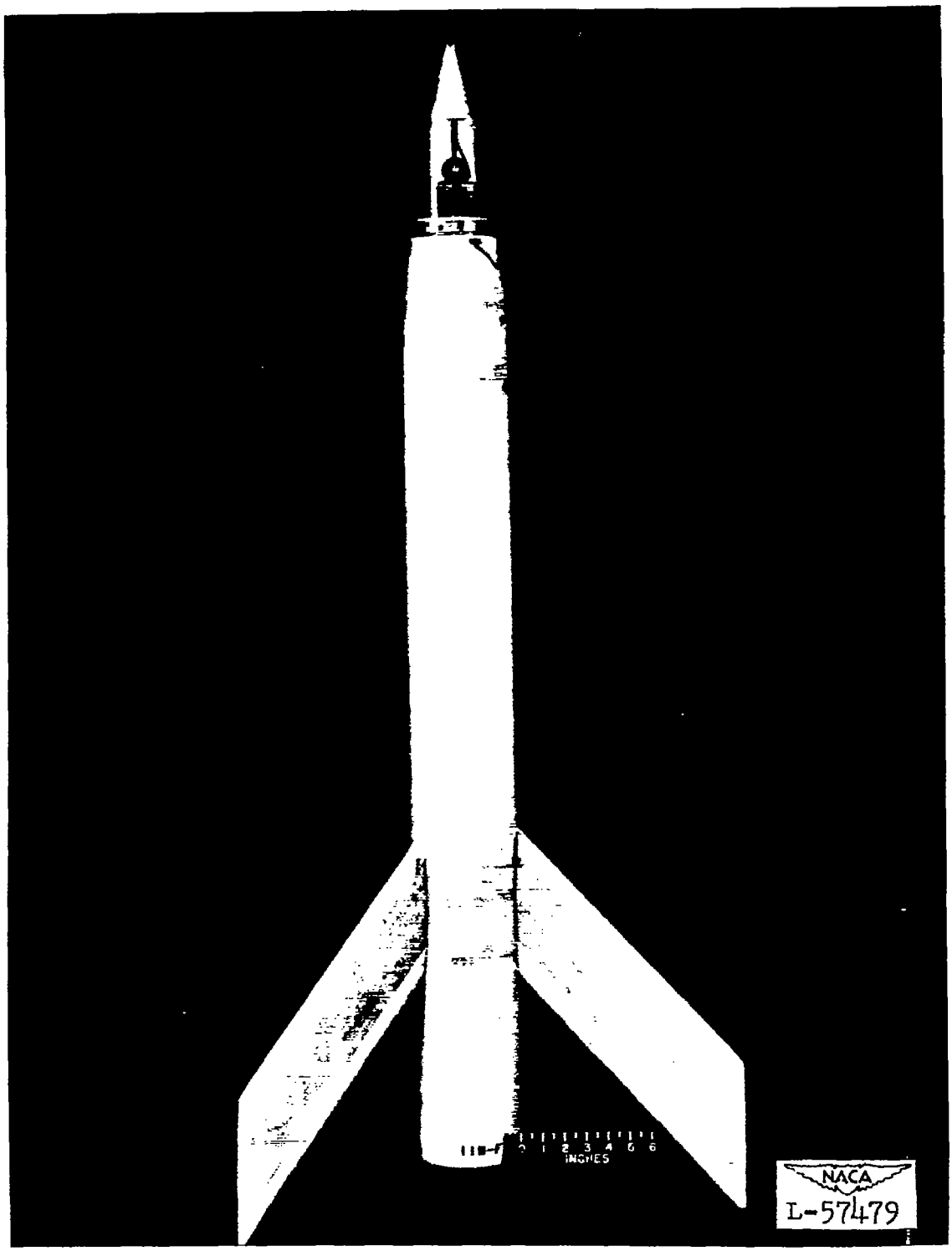

(b) $\Lambda = 45^{\circ}$.

Figure 2.– Concluded.

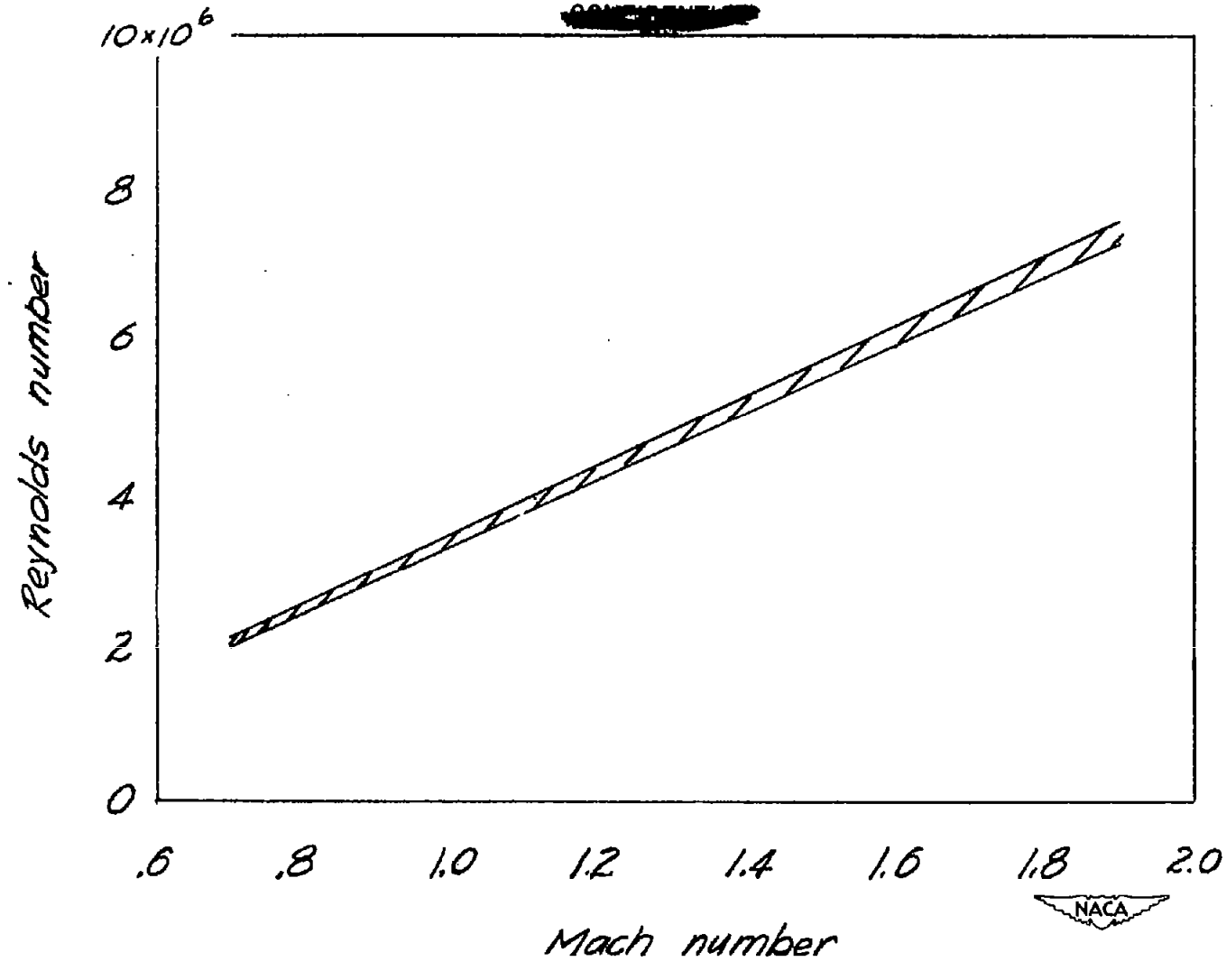

Figure 3.- Variation of Reynolds number with Mach number for range of climatic conditions encountered during tests.

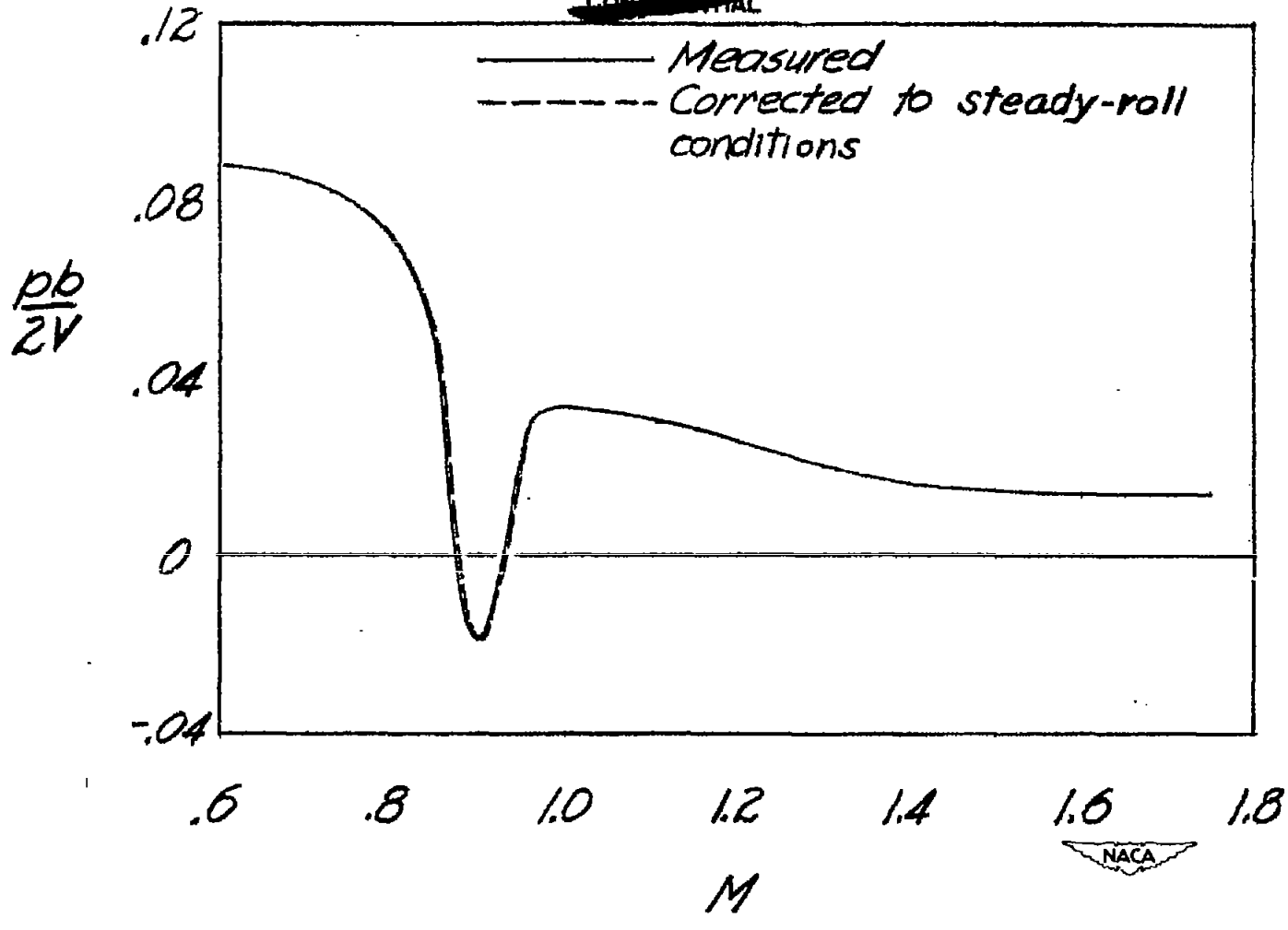

Figure 4.– Effect of moment of inertia about roll axis on measured variation of $\frac{pb}{2V}$ with Mach number.

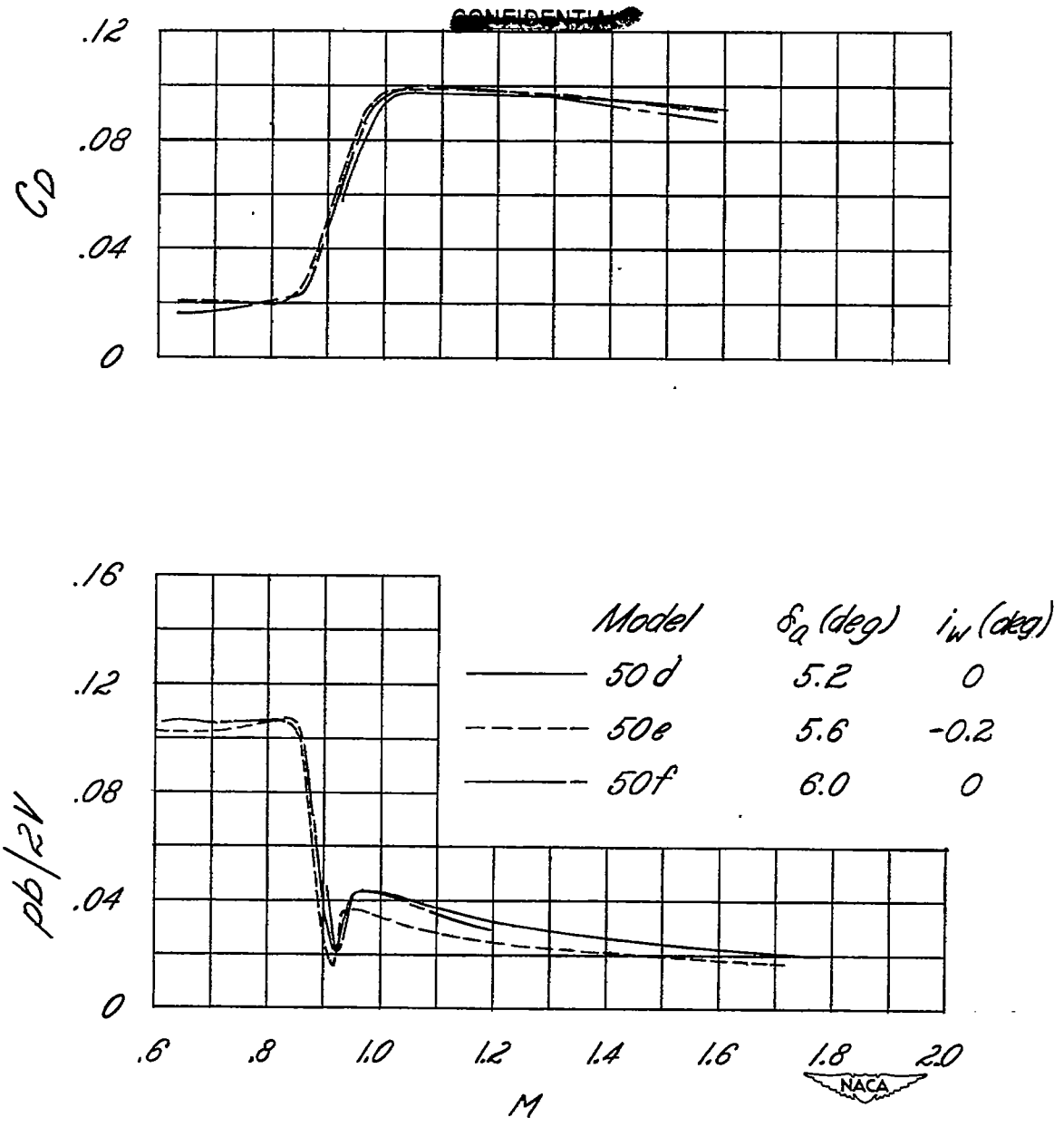

(a) NACA 65A009 airfoil section.

Figure 5.— Experimental results. $\Lambda = 0°$.

CONFIDENTIAL

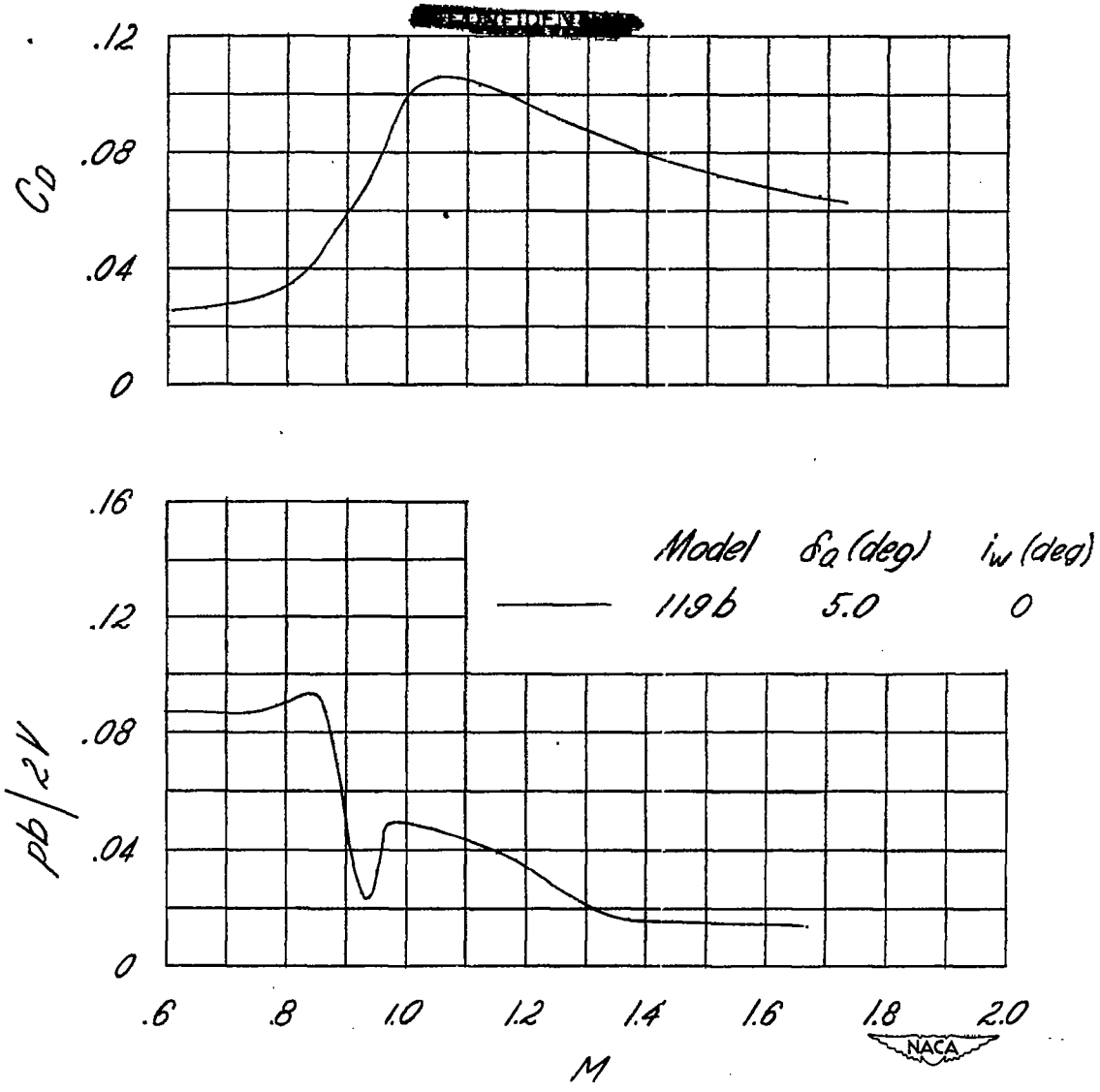

(b) 9-percent-thick double-wedge airfoil section.

Figure 5.- Continued.

CONFIDENTIAL

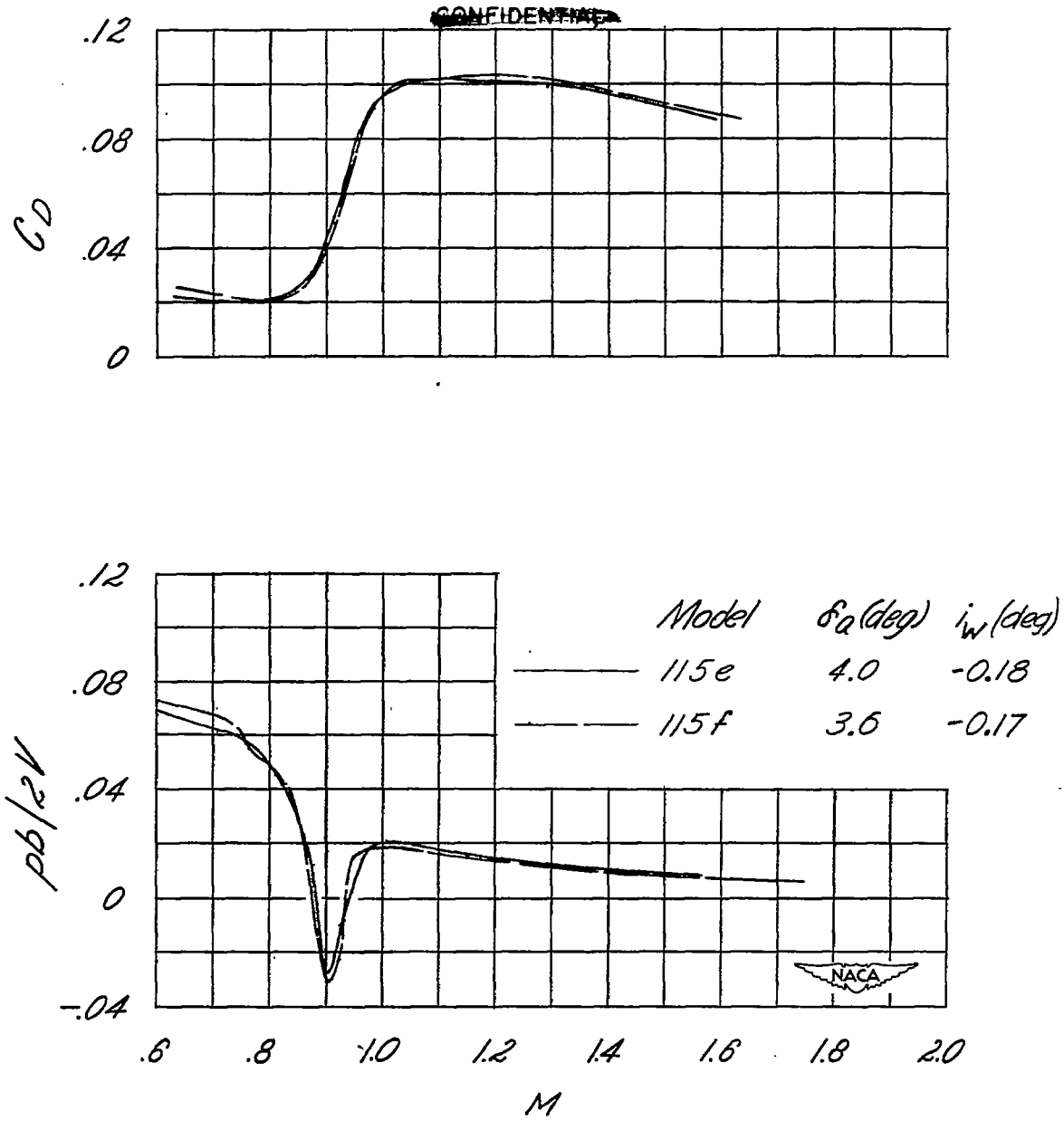

(c) NACA 16-009 airfoil section.

Figure 5.- Continued.

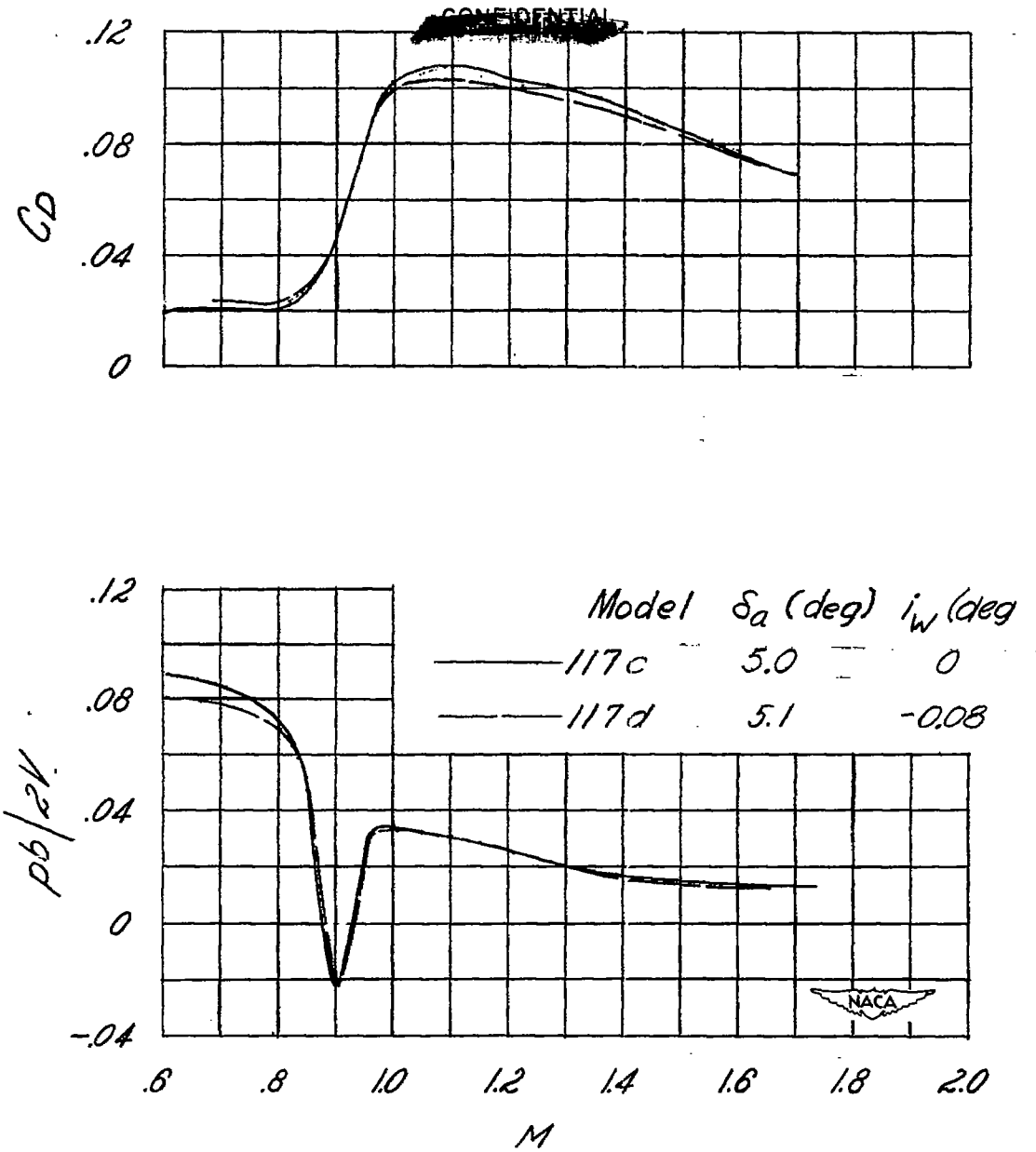

(d) 9-percent-thick circular-arc airfoil section

Figure 5.- Concluded.

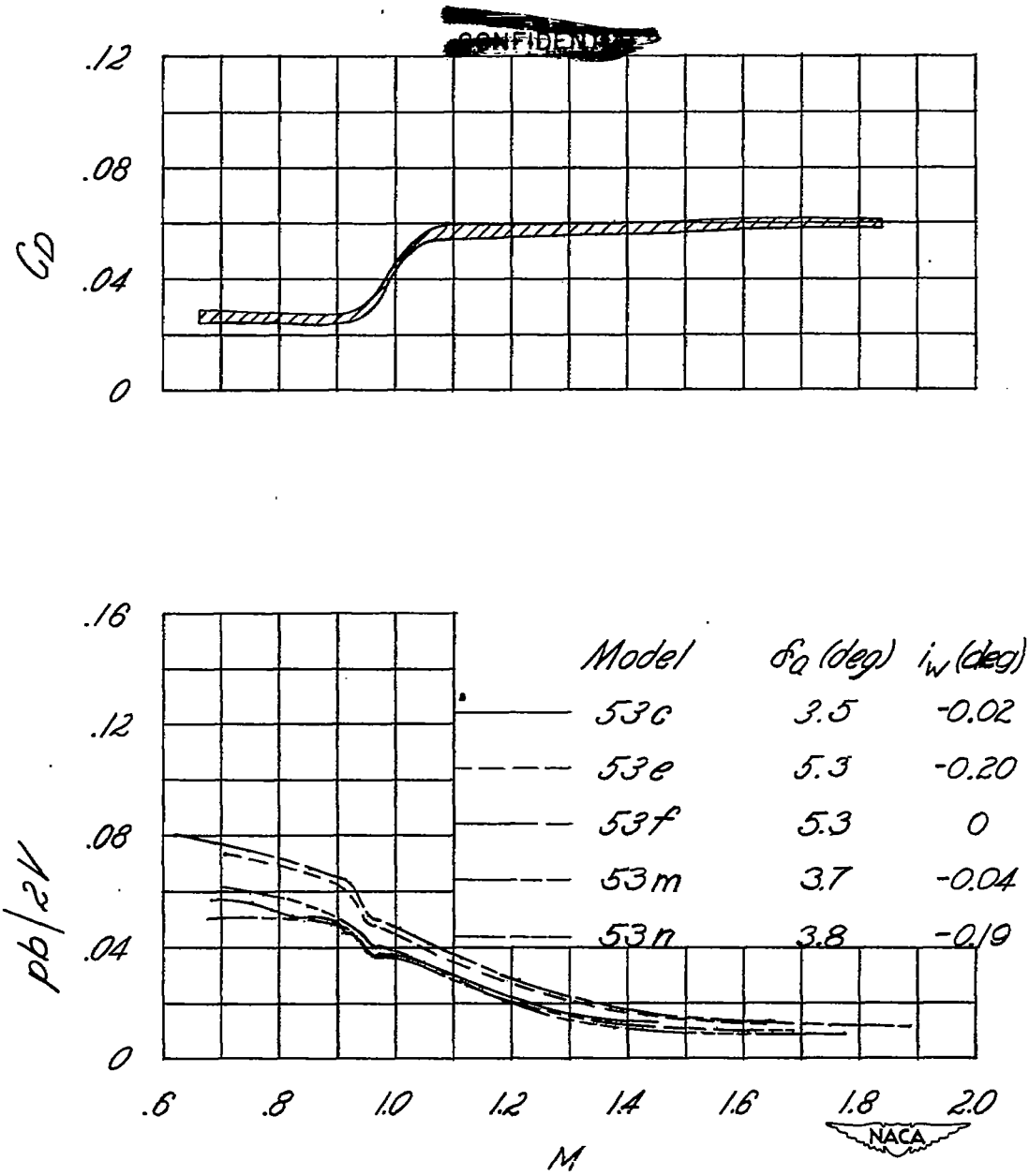

(a) NACA 65A009 airfoil section.

Figure 6.– Experimental results. $\Lambda = 45^\circ$.

CONFIDENTIAL

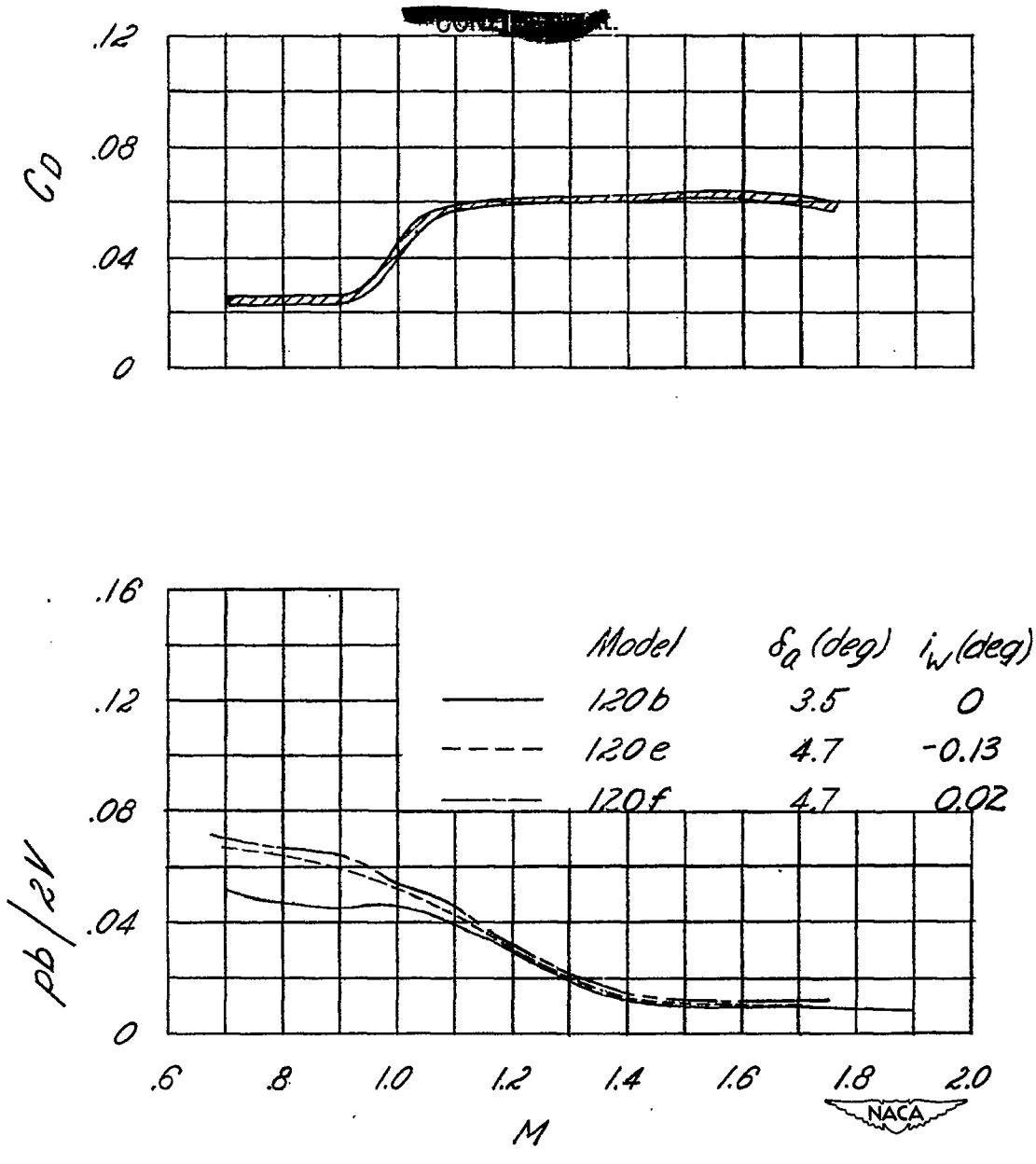

(b) 9-percent-thick double-wedge airfoil section.

Figure 6.- Continued.

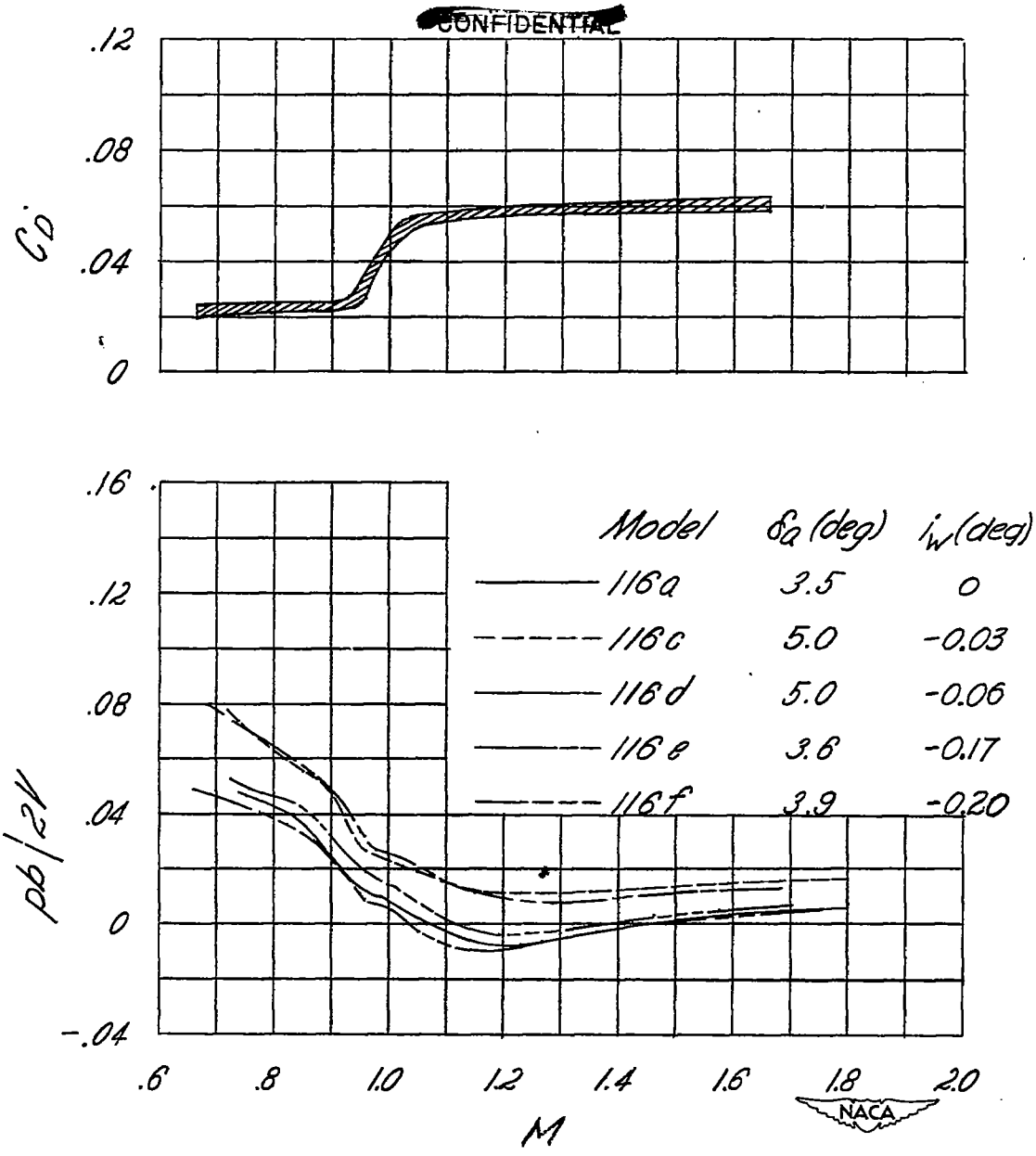

(c) NACA 16-009 airfoil section.

Figure 6.- Continued.

CONFIDENTIAL

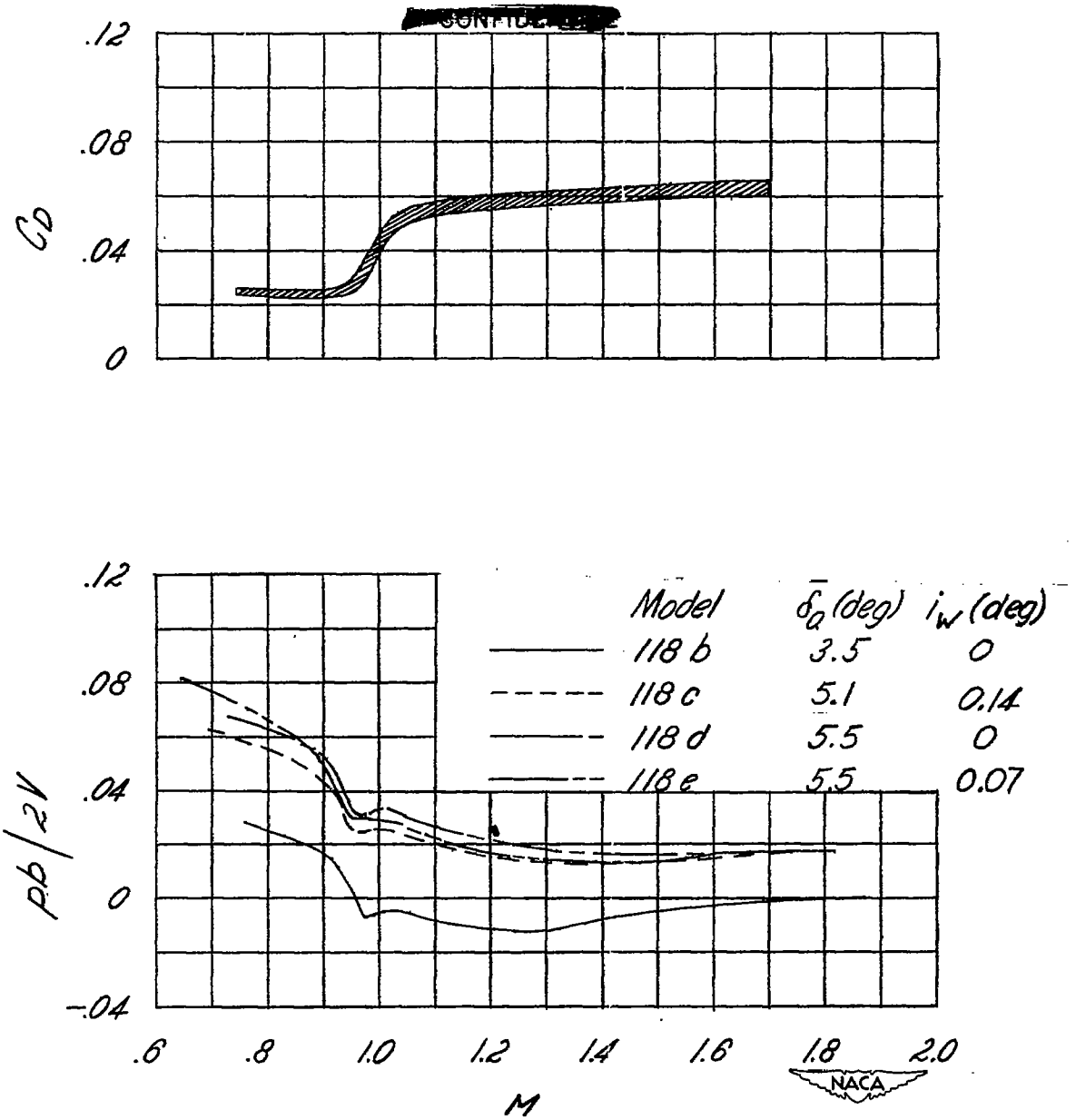

(d) 9-percent-thick circular-arc airfoil section.

Figure 6.- Concluded.

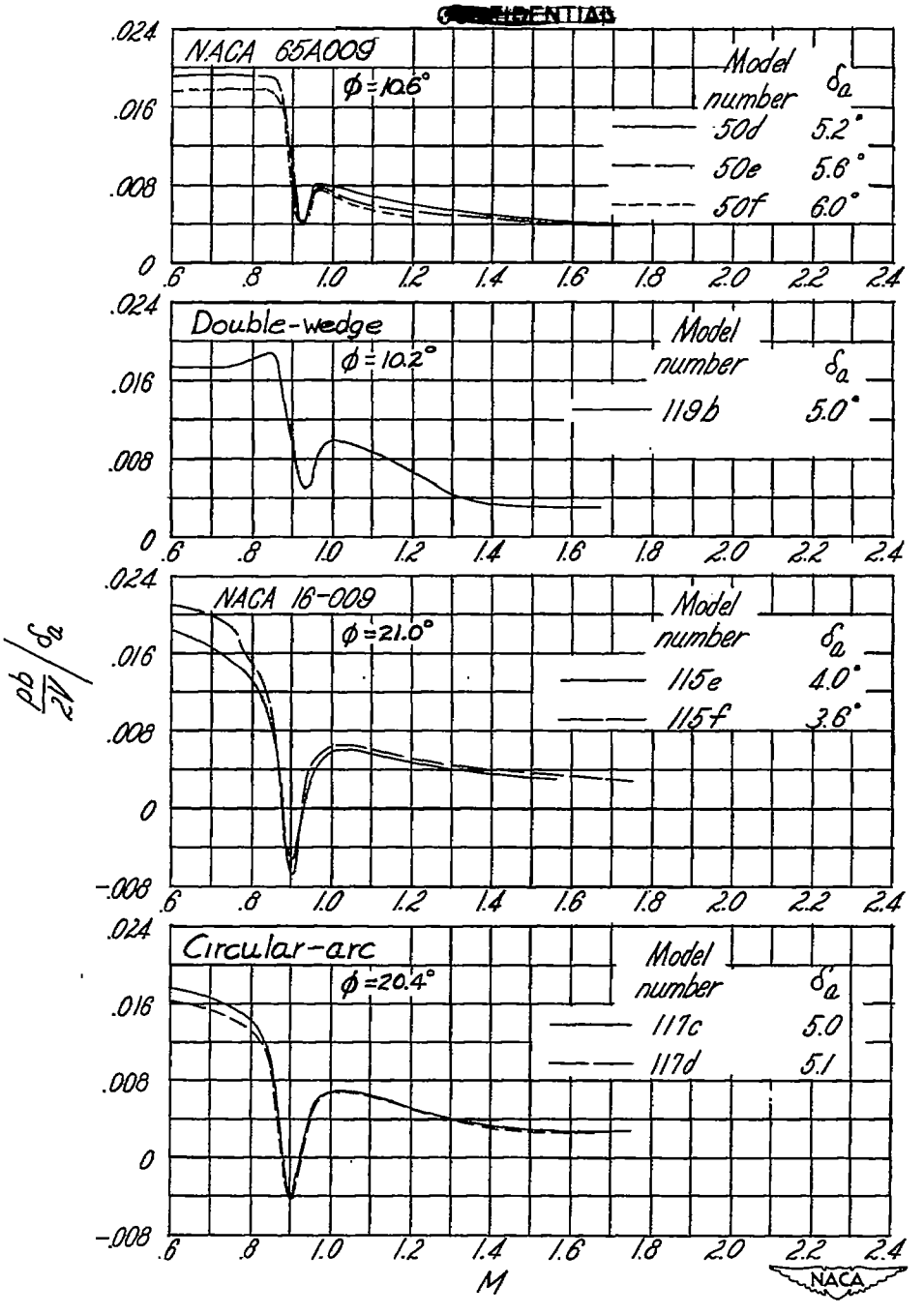

(a) $\Lambda = 0°$.

Figure 7.– Summary of wing–aileron rolling effectiveness results.

CONFIDENTIAL

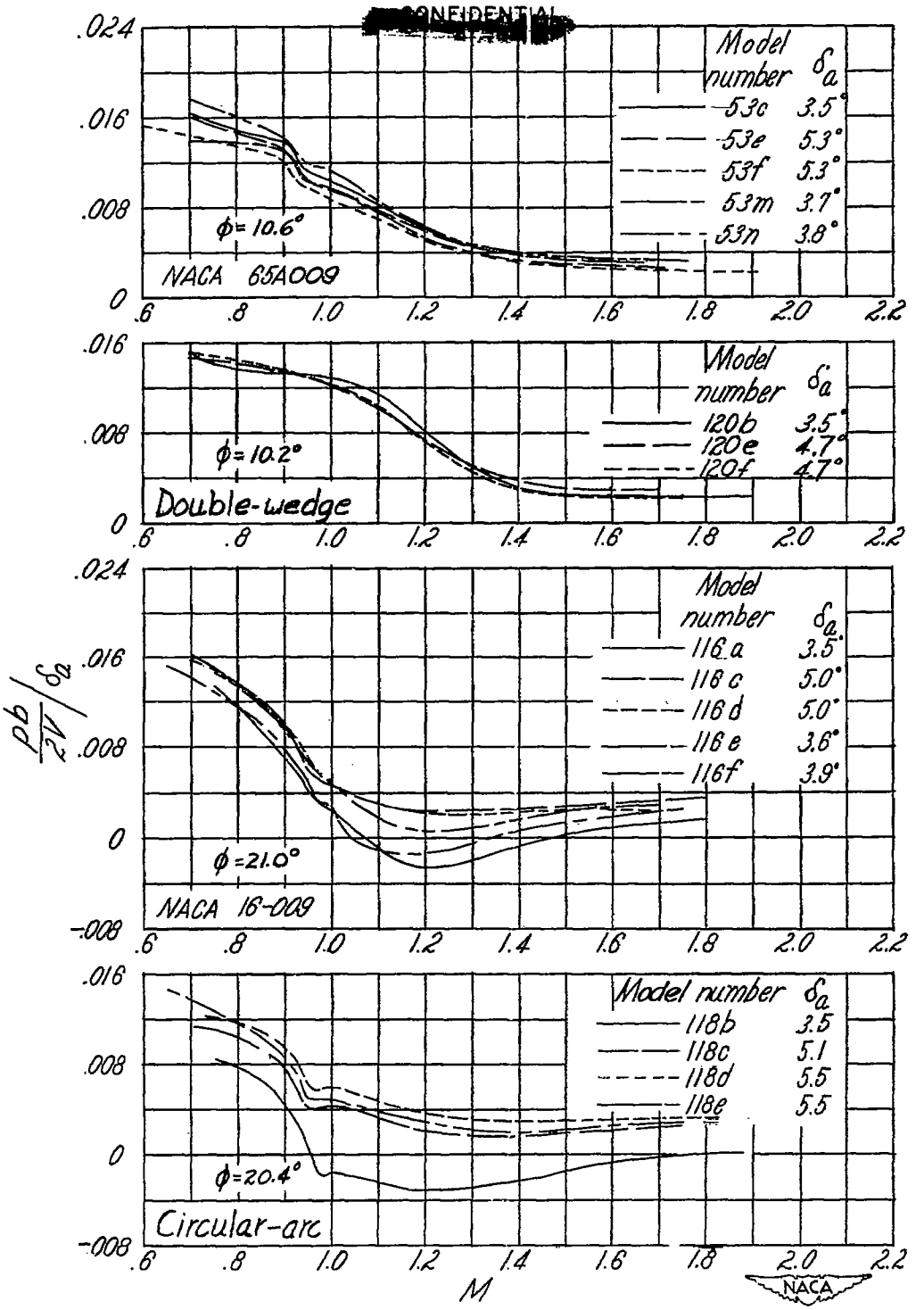

(b) $\Lambda = 45^{\circ}$.

Figure 7.— Concluded.

CONFIDENTIAL

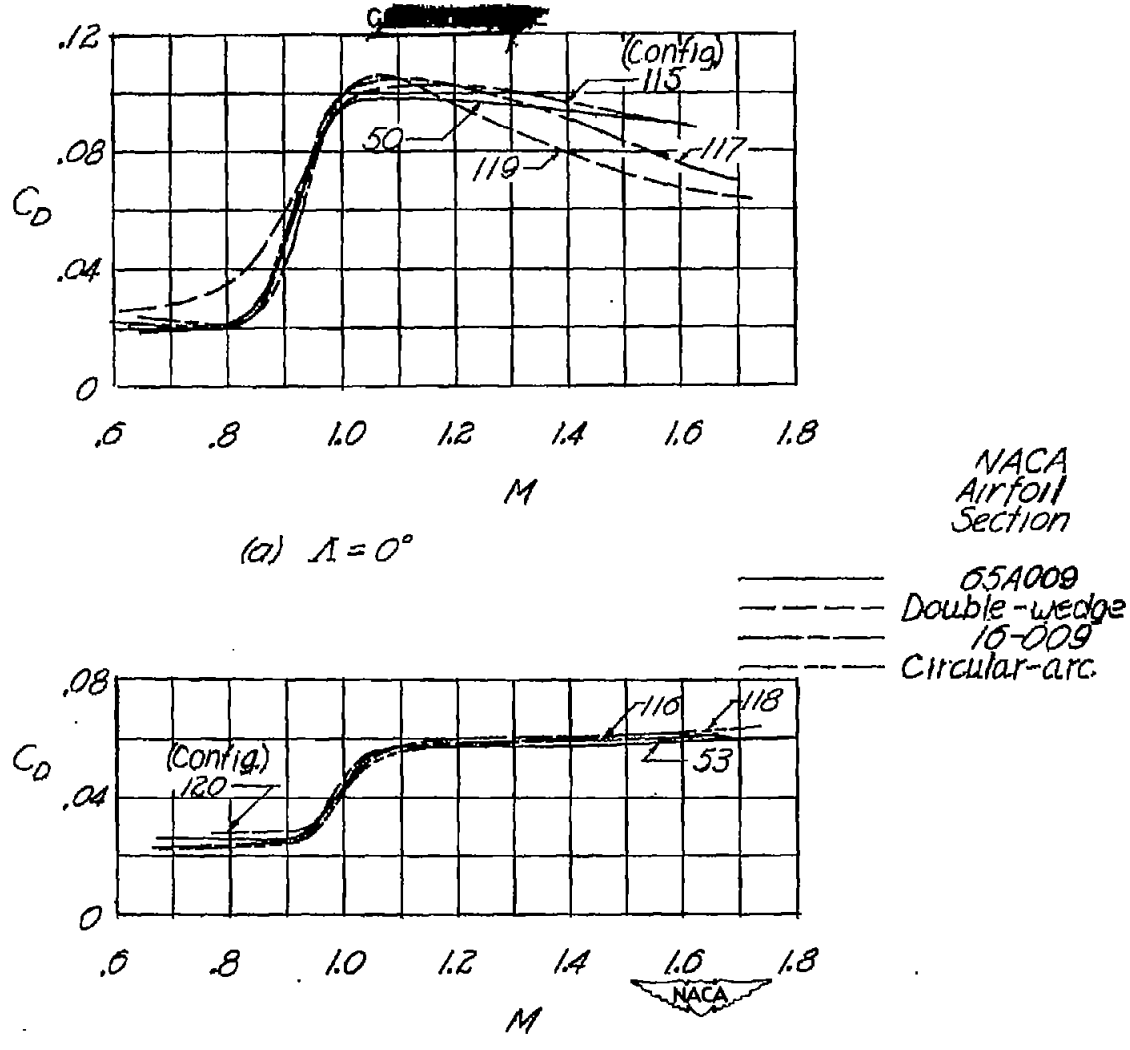

Figure 8.– Summary of drag results for each configuration.